ORNL/TM--8987

DE84 007564

Health and Safety Research Division

INITIAL ELECTRON ENERGY SPECTRA IN WATER IRRADIATED BY PHOTONS WITH ENERGIES TO 1 GeV

A. S. Todo
J. E. Turner
G. Hiromoto
R. N. Hamm
H. A. Wright

Date Completed - December 1983
Date Published - February 1984

Prepared by the
OAK RIDGE NATIONAL LABORATORY
Oak Ridge, Tennessee 37831
Operated by
UNION CARBIDE CORPORATION
for the
U.S. DEPARTMENT OF ENERGY
Office of Health and Environmental Research
Under Contract No. W-7405-eng-26

CONTENTS

ACKNOWLEDGMENTS

A. S. Todo and G. Hiromoto were guest scientists from the Instituto de Pesquisas Energéticas e Nucleares, São Paulo, S.P., Brazil. This research was also sponsored in part by the Deputy for Electronic Technology, Air Force Systems Command, under Interagency Agreement DOE No. 40-226-70.

INITIAL ELECTRON ENERGY SPECTRA IN WATER IRRADIATED BY PHOTONS WITH ENERGIES TO 1 GeV

A. S. Todo, G. Hiromoto, J. E. Turner, R. N. Hamm, and H. A. Wright

ABSTRACT

This work was undertaken to provide basic physical data for use in the dosimetry of high-energy photons. Present and future sources of such photons are described, and the relevant literature is reviewed and summarized. Calculations were performed with a Monte Carlo computer code, PHOEL-3, which is also described. Tables of initial electron and positron energies are presented for monoenergetic photons undergoing single interactions in water. Photon energies to 1 GeV are treated. The code treats explicitly the production of electron-positron pairs, Compton scattering, photoelectric absorption, and the emission of Auger electrons following the occurrence of K-shell vacancies in oxygen. The tables give directly the information needed to specify the absolute single-collision kerma in water, which approximates tissue, at each photon energy. Results for continuous photon energy spectra can be obtained by using linear interpolation with the tables. (Continuous spectra can also be used directly in PHOEL-3.) The conditions under which first-collision kerma approximate absorbed dose are discussed. A formula is given for estimating bremsstrahlung energy loss, one of the principal differences between kerma and absorbed dose in practical cases.

CHAPTER 1

INTRODUCTION

1.1 Objective of Study

Knowledge of the spectrum of initial energies of the electrons produced directly by photon interactions with matter is of fundamental importance for dosimetry, radiotherapy, radiochemistry, and understanding the biological effects of photons. Because the spectrum represents the basic physics that quantitatively describes the transfer of energy from the radiation field to matter, a number of investigators have compiled extensive spectral information. Cormack and Johns (CJ52) presented tables of the initial energy distributions of Compton and pair electrons produced in water irradiated by monoenergetic photons with energies from 10 keV to 25 MeV. Similar tables were given for photon energies up to 25 MeV by Johns and Laughlin (JL56), who included triplet production, which was ignored by Cormack and Johns. Given an initial photon spectrum, tables such as these can be used to estimate a number of important quantities for radiation protection, e.g., kerma (the sum of the initial kinetic energies of all charged particles liberated by indirectly ionizing particles per unit mass) and absorbed dose. Since water so closely approximates soft tissue in its response to photons, one thus obtains estimates of tissue kerma and dose.

The present study was undertaken to provide initial electron-energy spectra in water for photons with arbitrary energy spectra extending considerably above 25 MeV, where existing work leaves off. As described below, the Monte Carlo computer code PHOEL-3 was developed and used to tabulate such spectra for photon energies up to 1 GeV. In this introductory chapter we describe various sources of high-energy photons and recent interest in the associated radiation-protection problems. We also summarize previous work on electron-spectra compilations and their uses for dosimetry and then outline the plan for the work carried out here. Chapters 2 and 3 will describe the specific approach taken and the computer code that was developed. Chapter 4 presents the numerical results and discussion.

1.2 Sources of High-Energy Photons

In recent years sources of high-energy photons have become increasingly prevalent. The use of megavoltage x-rays in radiotherapy, for example, is now widespread. The National Council on Radiation Protection and Measurements in the United States issued a report in 1976 on shielding associated with the medical uses of X and gamma rays of energies up to 10 MeV (NC76). They issued another report in 1977 on radiation-protection guidelines for facilities with 0.1 to 100 MeV particle accelerators (NC-77). High-energy photons and neutrons often pose serious radiation-protection problems in such installations.

In higher-energy accelerators that can produce pions (e.g., proton synchrotrons with energies $\gtrsim$ 400 MeV), energetic photons occur from the decay of the neutral pion into two photons (lifetime $\sim 2 \times 10^{-16}$ s). In radiotherapy and in radiobiological experiments with stopping negative pions, for example, charge exchange produces low-energy neutral pions, π^0, which decay immediately into two 70-MeV photons emitted back-to-back. Photons with energies in the GeV range are produced as bremsstrahlung in electron accelerators.

Plans have been discussed for obtaining photon beams in the hundred GeV region at the Fermi National Accelerator Laboratory and at the European Organization for Nuclear Research, CERN (DM75). In a double-conversion scheme, photons from the π^0 particles produced by a 200-to-400-GeV proton beam can be converted into electron-positron pairs after magnetically sweeping away the charged particles present. An electron or positron beam of the desired momentum can then be selected for producing the high-energy photon beam by bremsstrahlung. Using a thin crystal as radiator gives a coherent bremsstrahlung spectrum with peaks of polarized photons.

High-energy photons are also present as a component of space radiation. They are of interest in this context not only for dosimetry, but also for their possible influence on the behavior of semiconductor communications materials (MC83).

1.3 Previous Work and Applications

The calculations of Cormack and Johns (CJ52) and of Johns and Laughlin (JL56), both for photons of energies to 25 MeV in water, were mentioned in

Section 1. For a number of years these have stood as basic references in photon dosimetry.

More recently, a Monte Carlo computer code, called PHOEL-2, was developed to calculate initial electron energies in water irradiated by photons with energies to 2 MeV (TH80). This code allows for the production of photoelectrons and Auger electrons, which were neglected in the earlier compilations (CJ52, JL56). The Auger electrons occur as a result of K-shell vacancies produced in oxygen. Since the K fluorescence yield of 0.0022 for oxygen (BT53, SW59) is small, it was assumed in the code that an Auger electron is emitted every time a K-shell vacancy occurs. PHOEL-2 thus calculates the initial energies of *all* electrons produced by the photons before the electrons start slowing down. PHOEL-2 is limited to photon energies no greater than 2 MeV because pair production is neglected. The code was used to calculate tables like those of Cormack and Johns up to 2 MeV (TH80), but with the addition of photoelectrons and Auger electrons. In an early version, PHOEL-2 was also combined with a Monte Carlo electron-transport code for liquid water for two studies in microdosimetry involving photons. In one investigation (HW78) spatial correlations of energy-deposition events were calculated. In the other (TH78), the yields of blobs, spurs, and short tracks (MM66) were calculated for X rays and for ^{60}Co gamma rays. Their possible bearing on interpreting observed photon RBE values at low doses (BM78) was considered. In another application, data for silicon were incorporated into PHOEL-2, and the spectra of initial electron energies in Si and SiO_2 were calculated for photons from ^{60}Co and for monoenergetic photons of energies to 2 MeV (TT82). This work was motivated by the interest in semiconductor devices as radiation detectors and their use as random-access-memory (RAM) units in the computers of satellites and space probes exposed to radiations in space (MC83).

The electron-transport studies in liquid water have recently been extended to later times. Following the initial electronic transitions, which are over in $\sim 10^{-15}$ s, the species present in water are the ions H_2O^+, excited molecules H_2O^*, and subexcitation electrons. The collective action of these species in liquid water was carried forward in time by Monte Carlo procedures to 10^{-11} s (TM80), which is approximately the

earliest time at which experimental observations are feasible. This time also marks the beginning of diffusion-controlled chemical reactions. The reactive species present at 10^{-11} s are OH, H_3O^+, H, O, and the hydrated electron. More recently, Monte Carlo calculations of the chemical diffusion and subsequent reactions were carried on to times of the order of 10^{-6} s, when all radical reactions within a single-electron track are complete (TM83). The experimental data most readily available for comparison are those for the Fricke dosimeter. The measured chemical yield (G-value) for conversion of ferrous to ferric ions for tritium beta rays (average energy, 5.6 keV) is 12.9 per 100 eV. In ref. TM83 the yield computed for 5-keV electrons by the formula

$$G(Fe^{3+}) = 2G_{H_2O_2} + G_{OH} + 3(G_H + G_e) \qquad (1.1)$$

was $G(Fe^{3+}) = 12.9$, where $G_{H_2O_2}$, G_{OH}, G_H, and G_e indicate, respectively, the calculated yields for H_2O_2, OH, atomic H, and the hydrated electron. While the precise numerical agreement between theory and experiment is perhaps fortuitous, it is nevertheless a desirable outcome of this work. The general merging of physics and chemistry in such studies was the subject of a 1982 Workshop at Argonne National Laboratory (AN82).

However, additional comparisons with experiment are badly needed. The most relevant data come from pulse radiolysis, which can measure yields of transient species to times down to the order of picoseconds. The observed decays of the hydrated electron and OH radical (JM76, JM77) are particularly pertinent, since these species are computed explicitly in the above-cited Monte Carlo calculations (TM83). Extension of the calculations, which have thus far not included bremsstrahlung, to the experimental electron energy range of 10 MeV is now in progress. PHOEL-3 will be used to handle the interaction of bremsstrahlung photons in this future work.

1.4 Basic Approach

As stated above, the objective of the present work is to obtain the initial electron energy spectra in water irradiated by high-energy photons. Such spectra could, in principle, be obtained by using existing computer

codes, such as the EGS System (cf., FN78 and references listed there) which was developed at the Stanford Linear Accelerator Center (SLAC). However, such systems are large, multipurpose codes designed principally for shielding calculations in thick, multiregion targets of various materials. They are, by many orders of magnitude, more elaborate and versatile than needed for the problem at hand. Their use entails detailed understanding of the codes and options as well as sophisticated computational facilities. It was decided, therefore, to explore the extension of the Monte Carlo work to higher energies, specifically for water, along the lines used in PHOEL-2. The result was the development of PHOEL-3, which can be used for photon energies to 1 GeV. As described below, the limiting energy is imposed by the approximations made in the treatment of triplet production. PHOEL-3 has been used to calculate the electron initial-energy tables presented here. These have also been published in the open literature (TH82a). Copies of the code PHOEL-3 are available from the Radiation Shielding Information Center, Oak Ridge National Laboratory, Oak Ridge, Tennessee 37831, USA (TH82b).

CHAPTER 2

INPUT DATA AND THEORY

This chapter describes the sources of the physical data used in PHOEL-3 and the processes treated--the photoelectric effect, Compton scattering, and pair and triplet production.

2.1 Photon Cross Sections in Water for Energies up to 1 GeV

The total mass attenuation coefficient μ/ρ and the Compton collision cross section σ_C for photons of different energies in water have been given by Evans (EV68). These values are shown in Table 2.1. The mass attenuation coefficients for the photoelectric effect, τ/ρ, and Compton collision, $\sigma_C N_o \rho$, which were derived from data given by Evans, are also included in Table 2.1. Here $N_o = 3.34 \times 10^{23}$ electrons/cm^3 and $\rho = 1$ g/cm^3 for water. The ratio τ/μ of the photoelectric and the total cross section used in PHOEL-3 is given in column 6. The last column in Table 2.1 shows, for comparison, the corresponding entries computed from values of σ and τ given in Cormack and Johns' paper (CJ52).

The numbers τ/μ in column 6 of Table 2.1 represent the probabilities that a photon of energy E will produce a photoelectron instead of being Compton scattered. A curve plotted through Evans' values is shown in Fig. 2.1 together with the points from Cormack and Johns' table. The differences arise from the larger photoelectric cross section used by Cormack and Johns. The Compton cross sections in Cormack and Johns and Evans agree, both having been obtained directly from the Klein-Nishina formula.

It is seen from Fig. 2.1 that linear interpolation between entries of Table 2.1 will give a good approximation to τ/μ if a few more points are included in regions where the curvature is large. The values used in PHOEL-3, obtained in this way, are given in Table 2.2, and linear interpolation is used to obtain τ/μ for values of photon energies between the entries.

Based on Evans' values, the photoelectric cross section was assumed to be negligibly small above 175 keV, and the total and Compton cross sections were assumed to be equal from 175 keV to 1 MeV.

Table 2.1. Compton and photoelectric mass attenuation coefficients for water

Photon energy E (keV)	Total attenuation μ/ρ (cm^2/g)	Compton collision cross section, σ_C (10^{-27} cm^2/electron)	Compton attenuation $\sigma_C N_o/\rho$ (cm^2/g)	Photoelectric attenuation τ/ρ (cm^2/g)	Present work τ/μ	(CJ52) τ/μ
10	4.99	640.5	0.214	4.78	0.958	0.957
15	1.48	629.0	0.210	1.27	0.858	
20	0.711	618.0	0.206	0.505	0.710	0.740
30	0.337	597.6	0.200	0.137	0.407	0.457
40	0.248	578.7	0.193	0.0547	0.221	0.266
50	0.214	561.5	0.188	0.0265	0.124	0.160
60	0.197	545.7	0.182	0.0147	0.075	0.099
80	0.179	517.3	0.173	0.00622	0.035	0.049
100	0.168	492.8	0.165	0.00340	0.020	0.024
150	0.149	443.6	0.148	0.000838	0.006	
200	0.136	406.5	0.136	0.000229	0.000	

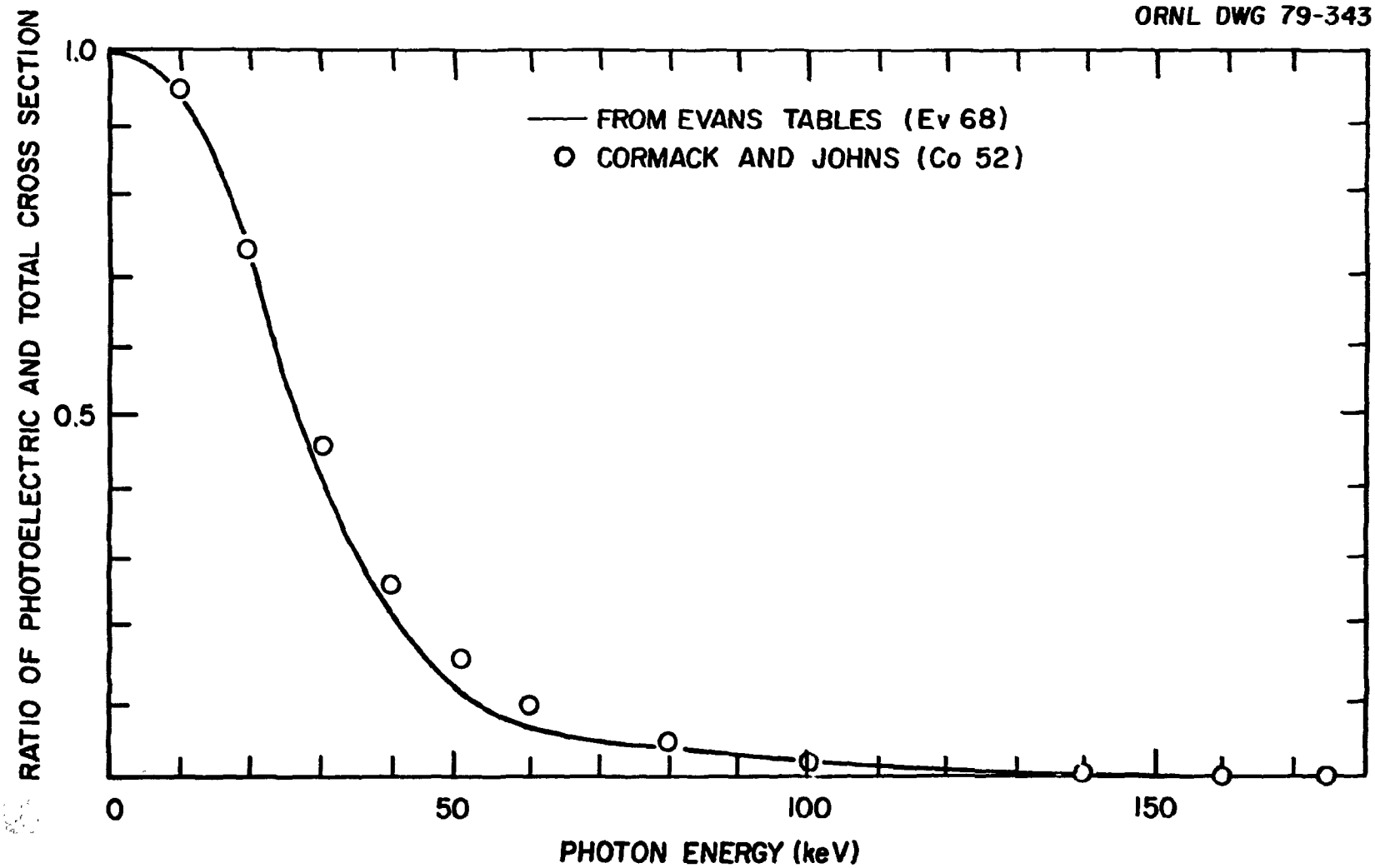

Fig. 2.1. Ratio of photoelectric and total cross sections as a function of energy for photons in water. The solid curve was computed from tables given by Evans (EV68), which provide the values used in PHOEL-3. For comparison, the points show some values given by Cormack and Johns (CJ52).

Table 2.2. Values used in PHOEL-3 for probability that a photon of energy E produces a photoelectron instead of being Compton scattered

Photon energy E (keV) E1(K)	Probability τ/μ F(K)	Photon energy E (keV) E1(K)	Probability τ/μ F(K)
0	1.00	45	0.167
5	0.995	50	0.124
10	0.958	55	0.0960
15	0.858	60	0.0750
20	0.710	80	0.0350
30	0.407	100	0.0200
35	0.300	150	0.0060
40	0.221	175	0.0000

The molecular cross sections for water at photon energies above 1 MeV are obtained from the tabulations of Hubbell, Gimm, and Overbo (HB80) for oxygen and hydrogen. They are shown in Table 2.3. The ratio $(\sigma_N + \sigma_E)/(\sigma_C + \sigma_N + \sigma_E)$ in the next-to-last column gives the probability that a photon will produce an electron-positron pair in the field of a nucleus or atomic electron instead of being Compton scattered. When pair production takes place, the ratio $\sigma_E/(\sigma_N + \sigma_E)$, shown in the last column, gives the probability that it happens in the field of an atomic electron rather than a nucleus. Because the atomic electron can recoil with appreciable energy, this process is called triplet production.

Table 2.4 presents values of the ratio $(\sigma_N + \sigma_E)/(\sigma_C + \sigma_N + \sigma_E)$ that are in sufficiently fine mesh, as a function of the photon energy E, to permit accurate linear interpolation. This table was obtained from a plot of the values given in Table 2.3. The same procedure was adopted to set up Table 2.5, which gives the value of $\sigma_E/(\sigma_N + \sigma_E)$. Linear interpolation between the entries given in Tables 2.4 and 2.5 is used in PHOEL-3.

Table 2.3. Molecular cross sections for water at photon energies above 1 MeV

Photon energy (MeV) EP(K), ET(K)	Compton, σ_C (barns)	Pair production: Nuclear field σ_N (barns)	Pair production: Electron field σ_E (barns)	Total $\sigma_C + \sigma_N + \sigma_E$ (barns)	$\frac{\sigma_N + \sigma_E}{\sigma_C + \sigma_N + \sigma_E}$ FP(K)	$\frac{\sigma_E}{\sigma_N + \sigma_E}$ FT(K)
1.022	2.090 + 00	0.000	0.000	2.090 + 00	0.0000	-
2.044	1.446 + 00	1.260 - 02	0.000	1.459 + 00	-	0.0000
3	1.153 + 00	3.342 - 02	4.035 - 04	1.187 + 00	0.0285	0.0118
4	9.620 - 01	5.420 - 02	1.647 - 03	1.018 + 00	0.0548	0.0287
5	8.306 - 01	7.271 - 02	3.283 - 03	9.066 - 01	0.0838	0.0434
6	7.343 - 01	8.935 - 02	5.041 - 03	8.287 - 01	0.1139	0.0530
8	6.066 - 01	1.175 - 01	8.504 - 03	7.266 - 01	0.1713	0.0684
10	5.116 - 01	1.406 - 01	1.170 - 02	6.639 - 01	0.2294	0.0768
15	3.786 - 01	1.837 - 01	1.835 - 02	5.807 - 01	0.3480	0.0910
20	3.039 - 01	2.150 - 01	2.357 - 02	5.425 - 01	0.4398	0.0989
30	2.212 - 01	2.591 - 01	3.135 - 02	5.117 - 01	0.5678	0.1080
40	1.758 - 01	2.894 - 01	3.594 - 02	5.011 - 01	0.6492	0.1130
50	1.467 - 01	3.126 - 01	4.144 - 02	5.007 - 01	0.7070	0.1170
60	1.264 - 01	3.309 - 01	4.503 - 02	5.023 - 01	0.7484	0.1200
80	9.971 - 02	3.587 - 01	5.063 - 02	5.090 - 01	0.8041	0.1240
100	8.276 - 02	3.790 - 01	5.487 - 02	5.166 - 01	0.8398	0.1270
150	5.894 - 02	4.129 - 01	6.224 - 02	5.341 - 01	0.8896	0.1310
200	4.621 - 02	4.337 - 01	6.711 - 02	5.470 - 01	0.9155	0.1340
300	3.275 - 02	4.588 - 01	7.337 - 02	5.649 - 01	0.9420	0.1380
400	2.565 - 02	4.735 - 01	7.729 - 02	5.764 - 01	0.9555	0.1400
500	2.124 - 02	4.832 - 01	8.001 - 02	5.845 - 01	0.9564	0.1420
600	1.819 - 02	4.902 - 01	8.204 - 02	5.904 - 01	0.9692	0.1430
800	1.420 - 02	4.997 - 01	8.490 - 02	5.988 - 01	0.9763	0.1450
1000	1.168 - 02	5.058 - 01	8.681 - 02	6.043 - 01	0.9807	0.1470

Table 2.4. Values used in PHOEL-3 for probability that a photon of energy E produces an electron-positron pair instead of being Compton scattered

Photon energy E (MeV) EP(K)	$\frac{\sigma_N + \sigma_E}{\sigma_C + \sigma_N + \sigma_E}$ FP(K)	Photon energy E (MeV) EP(K)	$\frac{\sigma_N + \sigma_E}{\sigma_C + \sigma_N + \sigma_E}$ FP(K)
1.022	0.000	45	0.6840
3	0.0285	50	0.7070
4	0.0548	60	0.7484
5	0.0838	80	0.8041
6	0.1139	100	0.8398
8	0.1713	150	0.8896
10	0.2294	200	0.9155
15	0.3480	300	0.9420
20	0.4398	400	0.9555
25	0.5080	500	0.9564
30	0.5676	600	0.9692
35	0.6140	800	0.9763
40	0.6492	1000	0.9807

Table 2.5. Values used in PHOEL-3 for probability that a photon of energy E undergoes triplet rather than pair production

Photon energy E (MeV) ET(K)	$\frac{\sigma_E}{\sigma_N + \sigma_E}$ FT(K)	Photon energy E (MeV) ET(K)	$\frac{\sigma_E}{\sigma_N + \sigma_E}$ FT(K)
2.044	0.0000	20	0.0989
3	0.0118	30	0.1080
4	0.0287	40	0.1130
5	0.0434	50	0.1170
6	0.0530	60	0.1200
7	0.0613	80	0.1240
8	0.0684	100	0.1270
9	0.0723	150	0.1310
10	0.0768	200	0.1340
11	0.0806	300	0.1380
12	0.0837	400	0.1400
13	0.0863	500	0.1420
14	0.0889	600	0.1430
15	0.0910	800	0.1450
16	0.0928	1000	0.1470
18	0.0960		

2.2 Treatment of the Photoelectric Effect

PHOEL-3 treats individual photons on a statistical basis. If the input photon energy is less than 175 keV, then the code picks a random number and decides by linear interpolation in Table 2.2 whether the photon is Compton scattered or produces a photoelectron.

The threshold energy for producing a K-shell vacancy in oxygen is 0.532 keV. If $E \geq 0.532$ keV, then a photoelectron of energy $T = E - 0.532$ is assumed to be emitted. Since the fluorescent yield from oxygen is very small, it is further assumed that creation of the K vacancy is followed

(immediately) by release of an Auger electron. The average L-shell binding energy in oxygen is about 0.012 keV. Therefore, the energy of the Auger electron is assumed to be 0.508 keV, the difference between the K-shell binding energy and twice the L-shell energy. If $0.532 > E > 0.012$ keV, then a photoelectron of energy $T = E - 0.012$ keV is assumed to be produced from the L shell. If $E < 0.012$ keV, nothing further happens to the photon; however, the total number and energy of these photons are tabulated.*

2.3 Treatment of Compton Scattering

The cross section $d\sigma/dT$ for producing Compton electrons of kinetic energy T is given by Eq. (26.7) of a review article by Evans (EV58):

$$\frac{d\sigma}{dT} = \frac{\pi r_o^2}{m_o c^2 \alpha^2}\left[2 + \left(\frac{T}{E-T}\right)^2\left(\frac{1}{\alpha^2} + \frac{E-T}{E} - \frac{2}{\alpha}\frac{E-T}{T}\right)\right]\frac{cm^2}{\text{keV electron}} . \qquad (2\text{-}1)$$

Here

$r_o = e^2/m_o c^2 = 2.18\times10^{-13}$ cm = classical electron radius

$m_o c^2 = 511$ keV = electron rest energy

T = kinetic energy of Compton electron

E = photon energy

$\alpha = E/m_o c^2$.

The unnormalized cumulative distribution $S(E,T)$ for producing a Compton electron of energy T or less is obtained by integrating Eq. (2-1). We find

$$S(E,T) = \int_0^T \frac{d\sigma}{dT}\,dT$$

$$= \frac{\pi r_o^2 T}{m_o c^2 \alpha^2}\left[\frac{2E - T}{2E} + \frac{2}{\alpha} + \frac{2E - T}{\alpha^2(E - T)} - \frac{E}{T}\left(1 - \frac{2}{\alpha} - \frac{2}{\alpha^2}\right)\ln\left(1 - \frac{T}{E}\right)\right] . \qquad (2\text{-}2)$$

*The probability is very small that the calculated energy after Compton scattering will be less than 0.012 keV. No such photons have turned up thus far in computations with PHOEL-3 involving a total of several hundred thousand photons.

The energy of the Compton electron can vary from zero to a maximum given by

$$T_{max} = \frac{2\alpha E}{1 + 2\alpha} . \tag{2-3}$$

Therefore, the normalized probability that a photon of energy E produces a Compton electron of energy T or less is given by

$$P(E,T) = \frac{S(E,T)}{S(E,T_{max})} . \tag{2-4}$$

The energy T of the electron produced by Compton scattering of a photon of energy E is obtained as follows in PHOEL-3. The quantity $S(E,T_{max})$ is first computed from Eqs. (2-2) and (2-3). A random number between 0 and 1 is selected for P, and the difference

$$D(E,T) = S(E,T) - P(E,T)S(E,T_{max}) \tag{2-5}$$

is formed. The transcendental equation

$$D(E,T) = 0 \tag{2-6}$$

is then solved for T by an iterative procedure.

The method of finding the solution of Eq. (2-6) in PHOEL-3 is straightforward. Since $0 < P < 1$, the function D(E,T) will be positive when $T = T_{max}$ and negative when $T = 0$. Furthermore, S(E,T) is a monotonic function of T for any E; and so D(E,T) changes sign exactly once in the interval $0 \leq T \leq T_{max}$, namely, at the point T_0 that is the root of Eq. (2-6). To find T_0 approximately, the code calculates D(E,T) successively at equally spaced points, starting with $T = 0.9\ T_{max}$ and proceeding to $0.8\ T_{max}$, etc., until the first negative value of D is obtained. (If D = 0, then the root has been found.) When D is first negative, T_0 lies within the last interval of length $0.1\ T_{max}$. This interval is subdivided into ten intervals of length $0.01\ T_{max}$, and the procedure is repeated in it to determine T_0 to within $0.01\ T_{max}$. This new interval is further subdivided to find T_0 to within an interval $0.001\ T_{max}$. The midpoint of this last interval is used for the value of T_0.

Whereas a photon of energy E disappears when it produces a photoelectron or an electron-positron pair, a photon of reduced energy (E - T) exists after Compton scattering. The option exists with PHOEL-3 to further trace the history of a photon after successive Compton scatterings until it disappears or to terminate the photon history after a single Compton scattering. With either option, the average energy of the first Compton electrons produced by photons from the input spectrum is compiled in the program. It is sometimes useful to have this average Compton energy as a check that this part of the program is operating properly.

It is assumed that all 10 electrons in the water molecule have equal probability for Compton scattering. Since there are two oxygen K-shell electrons per water molecule, there is a 20% probability that there will be a K vacancy following such an event. On this basis, PHOEL-3 selects a random number to decide whether a K-shell electron has been ejected after Compton scattering occurs. If so, then an Auger electron with energy 0.508 keV is also produced. The effects of electron binding on Compton scattering have been ignored in PHOEL-3. They modify the Compton cross section by no more than a few percent at photon energies of several tens of keV, where they are greatest (BN83).

2.4 Treatment of Pair and Triplet Production

Pair production. To compute the energy distribution of electrons and positrons from pair production in the field of a nucleus, we utilized data presented graphically by Bethe and Ashkin (BA53). In the nuclear field, the energy spectra of the electron and positron are the same. Bethe and Ashkin plot the cross section $[\Phi(E_+)/\bar{\Phi}](k - 2m_oc^2)$ for creation of a positron of total energy E_+ as a function of the kinetic energy $(E_+ - m_oc^2)$ of the positron divided by $(k - 2m_oc^2)$. Here $k = h\nu$ is the photon energy and m_oc^2 is the rest energy of an electron or positron. The function $\Phi(E_+)$ is given explicitly by Eq. (11) on page 326 of (BA53); Φ is the bremsstrahlung cross section, given by Eq. (61a) on page 265 of this reference. The dimensionless kinetic-energy parameter $x = (E_+ - m_oc^2)/(k - 2m_oc^2)$ is defined, and the probability $P(k,x)$ of producing a positron or electron with energy equal to or less than x is given by:

$$P(k,x) = \frac{\int_0^x [\Phi(E_+)/\bar{\Phi}](k - 2m_o c^2)dx}{\int_0^1 [\Phi(D_+)/\bar{\Phi}](k - 2m_o c^2)dx} . \qquad (2\text{-}7)$$

This normalized cumulative probability was evaluated numerically by integrating the curves plotted by Bethe and Ashkin. Since each curve is symmetric, the integral in the denominator was performed from 0 to 0.5. Therefore, the value of x, which is chosen from P(k,x) by random-number selection, can be assigned with equal probability to either a positron or electron. The function P(k,x), which is included in PHOEL-3 as input data, is presented in Table 2.6 for the same photon energies as Bethe and Ashkin's curves. For photons of other energies, linear interpolation is used between the values in Table 2.6. The probability P(k,x) appears in PHOEL-3 as PROB, the photon energy k as EPH, and the quantity x as ESL.

Triplet production. Following Bethe and Ashkin, we assume for triplet production that the recoil momentum q of the field electron is the same as it would be for a nucleus. Then its normalized distribution is given by (BA53):

$$P(q)dq = \frac{1}{A}\frac{dq}{q}\frac{m_o^2c^2}{m_o^2c^2 + q^2} \qquad (2\text{-}8)$$

for $q > q_{min}$, where $A = \ln(m_o c)/q_{min}$ and $q_{min} = m_o c(m_o c^2/k)$. Integrating, we find

$$P(q) = \int_{q_{min}}^{q} \frac{1}{A}\frac{dq}{d}\frac{m_o^2c^2}{m_o^2c^2 + q^2}$$

$$= 1 - \frac{1}{2\ln(k/m_o c^2)} \ln(1 + m_o^2c^2/q^2) , \qquad (2\text{-}9)$$

whereby the boundary conditions $P(\infty) = 1$ and $P(q_{min}) = 0$ are satisfied. Accordingly, the probability of producing a field electron of kinetic energy E; in units of $m_o c^2$ is

$$P(E') = 1 - \frac{1}{2\ln(k/m_o c^2)} \ln(1 + 1/E'^2) . \qquad (2\text{-}10)$$

Table 2.6. Probability distribution P(k,x)
defined by Eq. (7) for electron-positron energies in pair production

x \ k	2.000	3.000	4.000	6.000	10.00	20.00	40.00	80.00	200.0	2000
0.000	0.000	0.000	0.000	0.000	0.000	0.000	0.000	0.000	0.000	0.000
0.025	0.014	0.014	0.012	0.015	0.011	0.014	0.019	0.028	0.030	0.051
0.050	0.043	0.043	0.035	0.041	0.035	0.041	0.052	0.066	0.075	0.110
0.075	0.077	0.077	0.065	0.073	0.067	0.077	0.092	0.110	0.124	0.168
0.100	0.120	0.120	0.102	0.110	0.108	0.118	0.138	0.158	0.177	0.225
0.125	0.165	0.165	0.143	0.152	0.148	0.161	0.187	0.209	0.231	0.281
0.150	0.214	0.214	0.188	0.197	0.194	0.209	0.238	0.261	0.286	0.336
0.175	0.262	0.262	0.234	0.245	0.243	0.260	0.291	0.314	0.340	0.390
0.200	0.316	0.316	0.285	0.295	0.295	0.313	0.344	0.368	0.394	0.442
0.225	0.373	0.373	0.338	0.347	0.348	0.367	0.398	0.422	0.448	0.493
0.250	0.430	0.430	0.394	0.402	0.403	0.422	0.453	0.476	0.501	0.543
0.275	0.487	0.487	0.425	0.458	0.460	0.478	0.508	0.529	0.553	0.592
0.300	0.544	0.544	0.510	0.516	0.517	0.536	0.562	0.583	0.605	0.640
0.325	0.601	0.601	0.570	0.573	0.576	0.593	0.617	0.636	0.656	0.687
0.350	0.658	0.658	0.631	0.633	0.635	0.651	0.672	0.690	0.706	0.733
0.375	0.715	0.715	0.692	0.693	0.695	0.709	0.727	0.742	0.756	0.779
0.400	0.772	0.772	0.754	0.754	0.755	0.767	0.782	0.794	0.805	0.824
0.425	0.829	0.829	0.815	0.815	0.816	0.826	0.836	0.846	0.854	0.868
0.450	0.886	0.886	0.877	0.876	0.877	0.884	0.891	0.897	0.903	0.913
0.475	0.943	0.943	0.938	0.938	0.939	0.942	0.946	0.949	0.951	0.956
0.500	1.000	1.000	1.000	1.000	1.000	1.000	1.000	1.000	1.000	1.000

Solving for E', we obtain

$$E' = \frac{1}{(e^{B} - 1)^{\frac{1}{2}}} \qquad (2\text{-}11)$$

where $B = 2(1 - P)\ln(k/m_o c^2)$. The kinetic energy of the field electron in triplet production is obtained from Eq. (2-11) after random selection of P between 0 and 1.

We assume that the energy spectra of the positron and electron pair are the same as they would be in the field of a nucleus. The total kinetic energy to be shared between the pair is $(k - 2m_o c^2 - E')$, and their energies are computed as discussed above for pair production in the nuclear field.

As discussed by Bethe and Ashkin (BA53), this treatment of the recoil energy of the field electron in triplet production is only approximate. Accordingly, we have limited the use of PHOEL-3 to photon energies up to 1 GeV, where the triplet cross section is about 15% of the total cross section in water.

CHAPTER 3

DESCRIPTION OF CODE

The computer code PHOEL-3 was written in FORTRAN IV language, and its main purpose is to generate the initial electron energy distribution in water irradiated by photons. Although most numerical results will be presented for monoenergetic photons, an arbitrary spectrum can be used in PHOEL-3. In this chapter we briefly describe the code itself and how it operates (TH82b).

3.1 Listing of Numerical Data in PHOEL-3

The numerical data we have described for use in generating initial electron and positron energies are provided in PHOEL-3 by the sequential card images listed in Table 3.1. In running PHOEL-3, the user need not be concerned with this part of the package, unless he wishes to change the numerical data on which the calculations are based. In PHOEL-3, energies are expressed in keV throughout.

The numerical data contained on the first 17 cards listed in Table 3.1 are those given in Table 2.6. The next card specifies NBR, the number of lines in Table 2.2. In PHOEL-3, NBR = 16. The user could replace Table 2.2 by any set of values with NBR $\leq$ 101. The next 4 cards give the photon energies E1(K) and probabilities F(K) from Table 2.2. The number of lines used for specifying the pair-production cross section in Table 2.4, NBP = 26, is given on the next card, with the stipulation that NBP $\leq$ 101. The next 7 cards contain the photon energies EP(K) and the ratios FP(K) of the pair-production and total cross sections from columns 2 and 4 of Table 2.4. Next, NBT = 31 gives the number of lines used in columns 2 and 4 of Table 2.5 for specifying the ratio of the triplet and total pair-production cross sections, with NBT $\leq$ 101. The next 8 cards contain the energies ET(K) and ratios FT(K) for which these are given. The next card gives NTT, the number of pairs of energy and total cross section values, which are shown in Table 3.2. The last 1+ cards contain these energies and cross sections.

Table 3.1. Sequence of data cards in PHOEL-3 for calculation of electron-positron initial energies

Number of cards	Contents	Format	Remarks
2	EEL(J)	16F5.3	Electron kinetic energies divided by $(h\nu - 2m_0c^2)$; used for pair production from Table 2.6.
1	EPH(I)	10F8.4	Photon energies in units of m_0c^2; for pair production, from Table 2.6.
14	PROB(I,J)	16F5.3	Probabilities for pair electrons of different energies as a function of photon energy, from Table 2.6.
1	NBR	I3	Number of lines (16) in Table 2.2; NBR $\leq$ 101.
4	E1(K),F(K)	8F10.4	Energies and ratios of photoelectric and total cross sections (entries in Table 2.2).
1	NBP	I3	Number of lines used for specifying pair-production cross section (26 in Table 2.4); NBP $\leq$ 101.
7	EP(K),FP(K)	8F10.4	Energies and ratios of pair-production and total cross sections (columns 2 and 4 in Table 2.4.).
1	NBT	I3	Number of lines used for specifying ratio of cross section for triplet and total pair production (34 in Table 2.5); NBT $\leq$ 101.
8	ET(K),FT(K)	8F10.4	Energies and ratios of triplet and total pair-production cross sections (columns 2 and 4 in Table 2.5).
1	NTT	I3	Number of lines used for specifying total cross section (41 in Table 3.2); NTT $\leq$ 101.
1+	TXEN(I), XSECTT(I)	8F10.5	Energies and total cross sections for calculating absolute electron-positron energy spectra (Table 3.2).

Table 3.2. Total cross section for calculating absolute electron-positron energy spectra

Photon energy (MeV)	Total cross section (cm^2/g)	Photon energy (MeV)	Total cross section (cm^2/g)
0.010	4.994	5	0.03034
0.015	1.480	6	0.02776
0.020	0.7110	8	0.02425
0.030	0.3370	10	0.02219
0.040	0.2477	15	0.01946
0.050	0.2145	20	0.01818
0.060	0.1967	30	0.01711
0.080	0.1792	40	0.01678
0.100	0.1684	50	0.01671
0.150	0.1488	60	0.01683
0.200	0.1362	80	0.01703
0.300	0.1180	100	0.01727
0.400	0.1060	150	0.01787
0.500	0.09680	200	0.01825
0.600	0.08930	300	0.01890
0.800	0.07850	400	0.01926
1	0.07070	500	0.01951
1.5	0.05759	600	0.01971
2	0.04939	800	0.01997
3	0.03973	1000	0.02019
4	0.03407		

3.2 User's Input to PHOEL-3

The cards that the user supplies for operating PHOEL-3 are listed in Table 3.3. These determine the following quantities. The first card gives the number N of energy values used to specify the input photon spectrum, with $N \leq 101$. The N values of EN(I), PR(I), given next, are the energies and cumulative probabilities that represent the input photon spectrum. Photon and electron energies are expressed in keV throughout. One or more cards must be supplied here by the user. The pairs start with PR(1) = 1.0 at the highest photon energy EN(1). For a continuous photon spectrum, the pairs end with PR(N) = 0.0 at the lowest energy EN(N). The energy E of a photon from a continuous spectrum is selected randomly in PHOEL-3 from these pairs by linear interpolation. For monoenergetic photons, N = 1; and for ^{60}Co, N = 2. The input data for monoenergetic photons are given on a single card with PR(1) = 1.0 and EN(1) = E in keV. For ^{60}Co there is also only a single card, with PR(1) = 1.0 and EN(1) = 1332.0 and PR(2) = 0.5, EN(2) = 1173.0. Other spectra can be represented by specifying up to 101 pairs of values, starting with the highest energy. The user-supplied spectrum, which is read in SORSIN, is printed at the end of a run.

The card following the input photon spectrum specifies NCO, an integer of I1 format. If NCO = 1, PHOEL-3 will give a spectrum of photons of alternating energies EN(1) and EN(2). This scheme is appropriate for ^{60}Co, which emits equal numbers of photons at two energies. If this option is not desired, then some other integer (e.g., NCO = 0) must appear here.

The code maintains a tally of the numbers of photons it chooses from the input spectrum in various energy ranges. This is done to provide the spectrum of photons actually used in a calculation, which, of course, should agree statistically with the spectrum read into the code. A series of energy bins is set up for scoring the energy of a photon selected from the input spectrum. The next card in Table 3.3 gives NPBINS, the number of values of energy used to mark the boundaries between NPBINS-1 successive energy bins. The energy values PES(K) must be specified in the next 1+ cards, up to 100 bins being allowed ($NPBINS \leq 101$). The total number

Table 3.3. Input cards to PHOEL-3 supplied by the user

Number of cards	Contents	Format	Remarks
1	N	I3	Number of pairs of entries giving the input photon spectrum; N $\leq$ 101.
1+	EN(I),PR(I)	5F16.5	Energies and cumulative probabilities specifying the input photon spectrum.
1	NCO	I1	Set NCO = 1 for ^{60}Co and NCO = 0 for all other cases.
1	NPBINS	I5	Number of values used to specify energy bins for tabulating actual spectrum of input photons used in the calculations; NPBINS $\leq$ 101.
1+	PES(K)	8F10.0	Photon energies marking bin edges.
1	NEBINS	I5	Number of values used to specify energy bins for tabulating electron-positron energy spectrum; NEBINS $\leq$ 101.
1+	EES(K)	8F10.0	Electron energies marking bin edges.
1	IOPPHT	I3	IOPPHT = 1 includes photoelectric effect; IOPPHT = 0 shuts off photoelectric effect.
1	IOPSCT	I3	IOPSCT = 1 gives multiple Compton scattering; IOPSCT = 0 allows only single Compton scattering.
1	IOPABS	I3	IOPABS = 1 gives relative electron energy spectra; IOPABS = 0 gives absolute spectra per unit input photon fluence.
1	NPHOT	I6	Number of input photons.

of photons and the relative number in the various energy bins are tabulated and printed out at the end of the calculations. Only the energies of original photons chosen from the input spectrum are counted in this tabulation; the reduced energies of photons after Compton scattering are not.

An analogous set of NEBINS-1 bins is set up for tabulating the electron energy spectrum generated by PHOEL-3. This is done by specifying NEBINS ($\leq$ 101) on the next card and the electron energies EES(K) in keV on the next 1+ cards. The number of electrons/keV/photon from the input spectrum in each of the bins is tabulated and printed. The total number of electrons is also printed.

Several options are allowed in PHOEL-3, and these are chosen by the user by specifying integers on the next 3 cards. With IOPPHT = 1, the photoelectric effect is included in the calculations; when IOPPHT = 0, the photoelectric effect is shut off. When IOPSCT = 1, multiple Compton scattering can take place; and when IOPSCT = 0, only single scattering of an input photon can occur. When IOPABS = 1, only the relative electron energy spectra are computed; when IOPABS = 0, the absolute spectra per unit input photon fluence are calculated. Thus, the first-collision spectra are obtained by setting IOPSCT = 0 and IOPABS = 0.

The last card in the user-supplied data set specifies NPHOT, the number of photons to be used from the input photon spectrum.

In addition to the average energy of the first Compton electrons produced by the input photons mentioned above, the printout also includes the number and total energy of photons with E < 0.012 keV, the assumed oxygen L-shell ionization threshold, should any occur.

3.3 Operation of PHOEL-3

PHOEL-3 has six subroutines as shown in the flow diagram, Fig. 3.1. The subroutine SORSIN is called first, from which the data cards are read and some of the input information is printed. In addition to reading the input cards listed in Table 3.1, bins are set up in SORSIN for tabulating energies, and tallies IPN(L) for the number of photons in each bin are initialized to zero. Furthermore, IEN1(L), IEN2(L), IEN4(L), IEN5(L), IEN6(L) and IEN9(L) for the number of electrons in each bin are also

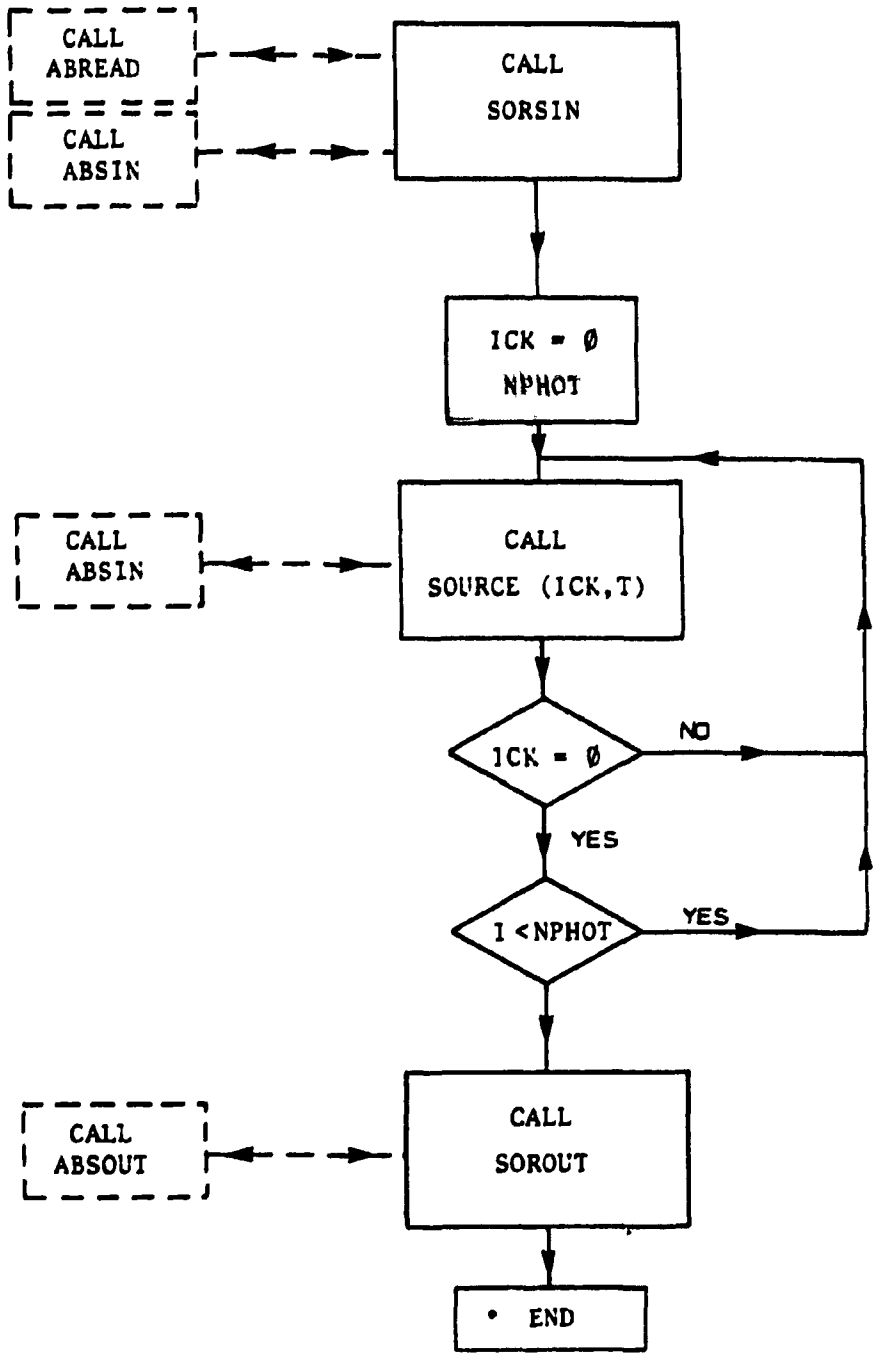

Fig. 3.1. Flow diagram of PHOEL-3.

initialized to zero. A monitor K2 that counts electrons is set equal to zero, as well as the number K1 and total ESUM of electrons with E < 0.012 keV. An integer ICO = 0 is specified, which generates photons of alternating energies if NCO = 1.

As seen in Fig. 3.1, SORSIN may call two other subroutines, ABREAD(IEBINS) and ABSIN(E), depending on the options chosen by the user. If the absolute electron spectra are desired, then the subroutine ABREAD(IEBINS) will be called by setting IOPABS = 0 (Table 3.3). This subroutine reads NTT, TXEN(I), and XSECTT(I) as listed in Table 3.3; it also initializes to zero the tallies EABS1(L), EABS2(L), EABS4(L), and EABS7(L) for the absolute number of electrons in each bin. If the input photon spectrum is monoenergetic (N = 1), the subroutine ABSIN is called from SORSIN. Otherwise, when N = 2 for ^{60}Co or N $\geq$ 3 for a continuous spectrum, ABSIN is called from the subroutine SOURCE. In ABSIN, the total cross section for a photon of energy E is obtained by linear interpolation between the values of Table 2.3. From this cross section, the probability (PROBB) that the photon will have a collision in a target of depth 1 cm is then calculated. When the input photon spectrum is monoenergetic (N = 1), this subroutine is called only once; but for ^{60}Co (N = 2) or a continuous spectrum, it is called for each new input photon. The value of PROBB printed at the end of the listing is meaningful only for monoenergetic photons. The absolute electron-positron spectra are calculated in PHOEL-3 only when single Compton scattering can take place.

As indicated in Fig. 3.1, the main program then sets another integer ICK = 0 and calls the subroutine SOURCE (ICK,T). This subroutine selects a photon of energy E from the input spectrum and returns to the main program with a value T for the energy of an electron it produces and a value for the integer ICK. The integer ICK = 0 indicates that a new photon will be chosen from the input spectrum when SOURCE is called again.

For input photon energies E < 1022 keV, below the pair-production threshold, the integer ICK = 1 indicates that a photon was Compton scattered and that the scattered photon of reduced energy will be treated next in SOURCE before another photon is selected from the input spectrum. As long as ICK = 1, the main program continues to go back to SOURCE for another electron energy without selecting another photon from the input

spectrum. After each Compton interaction, the program checks to see if the scattering occurred with a K-shell electron of oxygen, which happens 2/10 of the time. If so, then a 0.508-keV Auger electron will also be produced. In this case, the Compton electron energy T2 is computed and SOURCE returns to the main program with T2 and ICK = 4, indicating that there is a K-vacancy due to Compton scattering. The main program then calls SOURCE again, which produces the Auger electron of energy T9 = 0.508 keV and sets ICK = IOPSCT, with IOPSCT = 0 or 1, respectively, according to whether multiple or single Compton scattering has been selected. A photoelectron will eventually be produced. If it is from the L shell, then SOURCE returns to the main program with that photoelectron energy and ICK = 0, indicating that the photon is gone and that no more electrons will be produced until another photon is chosen from the input spectrum. If the photoelectron is from the K shell, then SOURCE returns to the main program with the electron energy and ICK = 2, indicating that there is a K vacancy. The main program then calls SOURCE again, which produces another (Auger) electron of energy 0.508 keV and sets ICK = 0, indicating that no more electrons will be produced by that original photon. (If a scattered photon should occur with energy < 0.012 keV, then SOURCE will return with ICK = 0.)

For photon energies E > 1022 keV, pair production in a nuclear field can take place; and for E > 2044 keV, triplet production in the field of an atomic electron is also possible. For a photon with $E \geq 1022$ keV, the code first decides whether it will undergo a Compton or pair-production interaction. A Compton-scattered photon is then treated as described above. With the option for multiple Compton scattering, the scattered photon is recycled. If pair production occurs, a check is made to see whether the photon energy is greater than 2044 keV. If E < 2044 keV, the energies of the positron and electron are computed, and the code returns to the main program with the electron energy T3 and ICK = 0. If $E \geq 2044$ keV, another check is made to decide whether pair or triplet production occurs. For a triplet event, the target-electron energy is calculated and SOURCE returns to the main program with the triplet-electron energy T6 and ICK = 3. The integer ICK = 3 indicates that a photon has interacted with an atomic electron. The main program then

calls SOURCE again, computes the energies of the pair electron and positron, and sets ICK = 0.

PHOEL-3 repeats this procedure until NPHOT photons from the input spectrum have been processed. SOROUT is then called, which tabulates and prints the statistical data generated. When the absolute electron spectra are calculated, ABSOUT is also called to tabulate and print the data generated.

PHOEL-3 also calculates the standard deviations in the absolute electron spectra according to Poisson statistics.

CHAPTER 4

RESULTS AND DISCUSSION

4.1 Selection of Data for Presentation

In this chapter we present tables of the initial energies of electrons and positrons produced in water irradiated by monoenergetic photons with energies up to 1 GeV. The data in the tables can be used with linear interpolation to calculate the spectra of initial electron and positron energies from photons with any specified spectrum up to 1 GeV. Only single photon interactions in the water are considered. The data are given in absolute terms so that one can obtain the first-collision kerma directly from the tables.

The output of PHOEL-3 lists separately the spectra of electrons and positrons resulting from photoelectric absorption, Compton scattering, Auger transitions, and pair and triplet production. For the last process, the energies of the triplet, "recoil" electron are also tabulated separately. Some grouping of the separate contributions has been made in the results presented here in order to reduce the amount of detail.

4.2 Statistical Considerations

Since PHOEL-3 utilizes Monte Carlo procedures, the calculated data are subject to inherent statistical uncertainties. The relative size of the statistical fluctuations can always be reduced by increasing the number of photons used in the computations. This procedure, of course, entails increased computer time and expense. A balance must be determined between acceptable levels of statistical uncertainty in the information obtained and practical costs. Generally, for most purposes in dosimetry and microdosimetry, accuracy of a few percent is adequate.

PHOEL-3 contains a subroutine that calculates the standard deviation, σ, and relative error, σ/x, for quantities x that are tabulated. Generally, as will be seen when the data are presented in the next section, the relative errors are of the order of a few percent. In some cases, a larger relative error was tolerated. In each table the largest relative errors occur for photons and electrons of the highest energies. It is in this energy range, also, that our treatment of triplet production may introduce comparable uncertainties.

4.3 Numerical Results

Table 4.1 gives the calculated spectra of initial energies of electrons produced in water irradiated by monoenergetic photons of energies from 10 to 220 keV. Only single photon interactions are allowed, and so the data give the "first-collision" spectra. Photoelectric absorption, which is the dominant physical process at the lower photon energies, decreases in importance with increasing photon energy. As seen from Fig. 2.1, the photoelectric effect is negligible above 175 keV. As described in Sections 2.2 and 2.3, the K-shell vacancy produced by photoelectric absorption or by Compton scattering results in the emission of a 0.508-keV Auger electron, the energy of which is included in the definition of kerma (IC80). These are the only physical processes that take place in the photon energy range covered in Table 4.1.

An example will illustrate the information provided in this and subsequent tables. For photons of energy 70 keV, for instance, Table 4.1 shows that there are 20.5×10^{-3} electrons/cm^3 per keV with initial energies in the range 0-5 keV per incident photon/cm^2. The multiplicative factor 10^{-3} is noted near the lower left in the table. This lowest energy range contains all Auger electrons and the Compton electrons of lowest energy. There are 8.60×10^{-3} electrons/(cm^3•keV) with initial energies in the range 5-10 keV and 11.5×10^{-3} electrons/(cm^3•keV) between 10 and 15 keV. All of these are Compton recoil electrons. In the next interval, 15-20 keV, there are 0.202×10^{-3} electrons/(cm^3•keV). This interval contains the kinematic maximum T_{max} = 15.1 keV for Compton electrons produced by 70-keV photons, as given by Eq. (2-3). For all entries the number of electrons is divided by the full width of the energy interval shown in the left-hand column of the table. The only electrons of higher energy produced by 70-keV photons are the photoelectrons. Table 4.1 shows that there are 1.40×10^{-3} electrons/(cm^3•keV) produced in the energy interval 65-70 keV per incident photon/cm^2. The total number of electrons/cm^3 per incident photon/cm^2 is found by multiplying each entry in the table by the size of the energy interval in which it occurs (= 5 keV) and adding. For 70-keV photons the result is 211×10^{-3} = 0.211, the number shown in the bottom line of the table. (The entries in the bottom lines of the tables are not to be multiplied by the factors indicated for the other table entries.)

Table 4.1. Initial electron-energy distribution in water (first-collision spectrum)

Number of electrons/(cm^3·keV) per photon/cm^2

Electron energy interval (keV)	Photon energy (keV)															
	10	20	30	40	50	60	70	80	90	100	120	140	160	180	200	220
0-5	201	108	64.2	47.1	31.7	24.7	20.5	17.4	15.2	13.6	11.3	9.58	8.44	7.63	7.03	6.61
5-10	188	0	0	3.79	13.8	12.2	8.60	6.97	6.13	5.22	4.27	3.37	2.69	2.18	1.80	1.47
10-15		0	0	0	0	5.40	11.5	6.73	5.06	4.48	3.53	2.84	2.44	2.08	1.75	1.51
15-20		70.2	0	0	0	0	0.202	8.02	5.85	4.11	3.08	2.58	2.13	1.78	1.57	1.37
20-25			0	0	0	0	0	0	5.91	5.16	2.90	2.34	1.97	1.72	1.42	1.28
25-30			21.8	0	0	0	0	0	0	4.51	3.11	2.16	1.79	1.61	1.41	1.20
30-35				0	0	0	0	0	0	0	3.87	2.19	1.67	1.46	1.32	1.17
35-40				8.82	0	0	0	0	0	0	3.52	2.40	1.67	1.36	1.21	1.11
40-45					0	0	0	0	0	0	0	2.97	1.77	1.29	1.13	1.03
45-50					4.17	0	0	0	0	0	0	3.55	1.91	1.32	1.08	1.00
50-55						0	0	0	0	0	0	0	2.29	1.39	1.08	0.935
55-60						2.38	0	0	0	0	0	0	2.79	1.56	1.10	0.915
60-65							0	0	0	0	0	0	1.10	1.80	1.14	0.912
65-70							1.40	0	0	0	0	0	0	2.15	1.27	0.914
70-75								0	0	0	0	0	0	2.28	1.41	0.974
75-80								0.919	0	0	0	0	0	0	1.63	1.04
80-85									0	0	0	0	0	0	1.94	1.17
85-90									0.601	0	0	0	0	0	1.27	1.24
90-95		MULTIPLY TABLE VALUES								0	0	0	0	0	0	1.51
95-100		BY 10^{-3}								0.341	0	0	0	0	0	1.72
100-110											0	0	0	0	0	0.360
110-250											0.00899	0.00583	0.00253	0	0	0
Avg. no. of electrons/cm^3 per photon/cm^2	1.94	0.891	0.430	0.298	0.248	0.224	0.211	0.200	0.194	0.187	0.179	0.171	0.164	0.158	0.153	0.149

Generally, 25,000 interactions at each photon energy were used to compute the electron spectra. The relative errors for the calculated values in Table 4.1 are ∿3% at 200 keV and less at the lower energies.

Table 4.2 presents the single-collision electron spectra for photon energies from 300 to 3000 keV. Compton scattering predominates in this energy range, the threshold energy for pair production being 1022 keV. The relative errors in the values in Table 4.2 vary from <5% for electron energies below 100 keV up to 10-20% for the relatively rare electrons with energies above 1000 keV at the highest photon energy of 3000 keV. Table 4.3 gives the spectra for photon energies from 4 to 25 MeV, the relative errors all being <4%. Table 4.4 covers photon energies from 30 to 1000 MeV. The relative errors for this table are no more than a few percent, except for electrons in the range 1-10 MeV for 500-MeV photons and 1-50 MeV for 1000-MeV photons. The relative errors for these entries are ∿5-8%.

In some applications it may be desirable to assess the separate contributions of Compton and pair electrons to the total spectrum of initial electron energies. Table 4.5 shows the spectra of initial energies of Compton electrons produced by photons with energies from 4 to 25 MeV. The relative errors are <3% below 10 MeV and <8% everywhere else. Table 4.6 extends the Compton electron spectra to photon energies of 1000 MeV; relative errors here are <10%. The separate positron spectra are given in Tables 4.7 and 4.8. The relative errors in both tables are <5% except for the positrons with initial energies below 100 MeV produced by 1000-MeV photons. The errors there are ∿5-18%. The spectra for pair electrons are the same as those for positrons, except for the addition of the relatively low-energy recoil electrons that occur in triplet production.

Together, these tables provide detailed information on the initial energies of electrons and positrons produced in water by single collisions of monoenergetic photons in the energy range from 10 keV to 1 GeV. They can be used to obtain the initial electron energy spectra for an arbitrary photon spectrum in this energy range by linear interpolation. The table entries, given in electrons/(cm^3•keV) or positrons/(keV•cm^3) per incident photon/cm^2, are absolute. Since Auger electrons are included, the values calculated are proportional to the single-collision kerma.

Table 4.2. Initial energy distribution of total number of electrons and positrons in water (first-collision spectrum)
Number of electrons/(cm^3·keV) per photon/cm^2

Electron energy interval (keV)	Photon energy (keV)					
	300	500	750	1000	2000	3000
0-10	3100	2170	1720	1460	979	769
10-20	801	310	146	77.8	21.4	8.10
20-30	807	314	146	84.6	25.8	12.6
30-40	703	290	126	72.9	21.8	7.01
40-50	673	297	136	87.9	18.3	10.8
50-60	638	307	141	72.9	23.1	7.63
60-70	619	296	130	77.0	16.8	6.70
70-80	570	271	141	78.6	22.6	11.2
80-90	522	258	136	84.4	24.9	10.9
90-100	524	253	146	76.7	21.0	9.35
100-200	440	238	127	77.8	21.1	10.2
200-300		255	119	71.8	21.3	10.0
300-400		136	113	72.5	22.5	9.85
400-500			142	70.3	21.9	10.1
500-600			139	72.4	21.1	10.8
600-700				92.7	21.3	10.8
700-800				145	20.5	10.3
800-900					21.2	11.5
900-1000					22.8	10.3
1000-1200					22.6	11.2
1200-1400					25.5	11.0
1400-1600					34.4	11.4
1600-1800	MULTIPLY TABLE VALUES BY 10^{-6}				53.7	12.1
1800-2000						12.4
2000-2400						15.7
2400-2800						29.5
Avg. no. of electrons/cm^3 per photon/cm^2	0.133	0.111	0.0936	0.0819	0.0583	0.0476

Table 4.3. Initial energy distribution of total number of electrons and positrons in water (first-collision spectrum). Number of electrons/(cm^3·MeV) per photon/cm^2

Electron energy interval (MeV)	Photon energy (MeV)													
	4	5	6	7	8	9	10	12	14	16	18	20	22	25
0-1	127	99.2	83.4	71.7	63.1	57.1	52.2	48.1	42.6	38.8	36.3	33.5	33.9	32.0
1-2	70.5	49.6	37.6	31.1	26.2	22.6	19.6	16.3	13.7	11.7	10.0	8.73	9.01	7.91
2-3	82.8	54.4	40.8	33.6	27.4	24.3	21.3	17.4	15.1	13.4	11.5	10.4	9.98	8.75
3-4	137	65.4	44.1	35.2	30.2	26.1	23.2	18.3	15.0	12.9	12.1	11.1	10.3	9.40
4-5		111	56.5	39.3	30.9	26.9	24.7	18.5	16.3	14.2	12.2	10.9	10.0	8.91
5-6			92.3	48.3	33.7	28.7	24.3	18.8	16.2	14.3	13.3	12.1	10.4	9.09
6-7				80.1	43.0	30.7	25.3	19.5	16.1	14.6	12.7	12.3	10.8	9.52
7-8					69.0	38.3	27.7	20.5	16.9	14.4	13.4	11.5	10.3	9.65
8-9						61.7	34.2	21.9	17.0	14.9	13.0	12.4	10.2	9.56
9-10							55.6	24.4	17.8	14.6	13.7	12.3	10.3	9.14
10-11								30.5	19.2	16.0	13.2	12.7	10.4	9.77
11-12								47.9	21.7	15.7	14.4	12.2	10.6	9.28
12-13									26.1	17.5	14.3	12.8	10.7	9.36
13-14									40.7	19.0	14.8	13.3	10.7	10.0
14-15										22.0	15.6	12.7	11.5	9.70
15-16										36.5	16.9	13.7	11.9	9.82
16-17											19.5	14.5	11.7	10.3
17-18											32.5	14.3	13.1	10.5
18-19												17.5	13.9	10.6
19-20												28.9	14.4	10.7
20-21	MULTIPLY TABLE VALUES BY 10^{-4}												18.1	12.0
21-22													26.3	12.2
22-23														12.9
23-24														16.1
24-25														23.2
Avg. no. of electrons/cm^3 per photon/cm^2	0.0417	0.0379	0.0355	0.0339	0.0323	0.0316	0.0308	0.0302	0.0294	0.0291	0.0289	0.0288	0.0289	0.0290

Table 4.4. Initial energy distribution of total number of electrons and positrons in water (first-collision spectrum). Number of electrons/(cm^3·MeV) per photon/cm^2

Electron energy interval (MeV)	Photon energy (MeV)							
	30	50	75	100	250	500	750	1000
0-1	29.8	27.1	25.3	25.3	27.1	28.0	29.1	30.0
1-5	7.35	4.86	3.12	2.21	1.43	0.680	0.489	0.370
5-10	8.04	5.43	3.76	2.74	1.44	0.631	0.356	0.369
10-20	8.34	5.27	4.00	3.13	1.53	0.717	0.407	0.233
20-30	10.9	5.17	3.88	3.14	1.55	0.809	0.456	0.292
30-40		5.56	3.82	3.16	1.56	0.797	0.498	0.340
40-50		7.27	3.89	3.10	1.45	0.803	0.507	0.322
50-60			4.13	3.14	1.44	0.857	0.559	0.381
60-70			4.38	3.20	1.37	0.826	0.563	0.393
70-80			2.71	3.23	1.41	0.824	0.558	0.387
80-90				3.35	1.25	0.801	0.516	0.441
90-100				3.60	1.28	0.755	0.562	0.401
100-200					1.31	0.740	0.543	0.424
200-300					0.819	0.688	0.513	0.407
300-400						0.743	0.492	0.402
400-500						0.830	0.493	0.389
500-600	MULTIPLY TABLE VALUES						0.533	0.389
600-700	BY 10^{-4}						0.561	0.403
700-800							0.250	0.407
800-900								0.427
900-1000								0.365
Avg. no. of electrons/cm^3 per photon/cm^2	0.0292	0.0306	0.0325	0.0338	0.0381	0.0406	0.0418	0.0422

Table 4.5. Initial Compton electron-energy distribution in water (first-collision spectrum)

Number of electrons/(cm^3·MeV) per photon/cm^2

Electron energy interval (MeV)	Photon energy (MeV)													
	4	5	6	7	8	9	10	12	14	16	18	20	22	25
0-1	116	88.0	72.3	61.0	52.6	46.8	42.2	36.3	31.5	27.5	24.8	22.2	20.7	18.5
1-2	55.2	35.0	23.4	17.7	13.5	10.5	8.44	5.70	4.10	3.27	2.60	2.16	1.84	1.45
2-3	72.0	39.7	26.2	18.9	13.5	10.6	8.61	5.95	4.53	3.33	2.65	2.18	1.77	1.34
3-4	137	55.9	30.2	20.5	15.2	11.5	9.07	6.42	4.37	3.36	2.78	2.05	1.80	1.45
4-5		111	47.7	26.1	17.0	12.4	10.1	6.70	5.20	3.44	2.59	2.26	1.86	1.29
5-6			92.3	40.0	21.4	15.1	10.3	6.93	4.79	3.96	2.85	2.22	1.82	1.40
6-7				80.1	35.7	18.9	12.7	7.66	5.22	3.75	2.95	2.37	1.96	1.35
7-8					69.0	31.6	17.0	8.50	5.59	4.11	2.95	2.46	1.97	1.57
8-9						61.7	28.3	10.6	5.86	4.13	3.33	2.25	2.04	1.64
9-10							55.6	14.1	7.28	4.25	3.31	2.62	1.88	1.59
10-11								23.9	8.79	5.33	3.41	2.63	2.32	1.53
11-12								47.9	12.4	6.05	3.96	3.11	2.23	1.60
12-13									20.7	7.56	4.63	2.81	2.56	1.65
13-14									40.7	10.9	5.56	3.52	2.32	1.86
14-15										17.4	6.84	4.04	2.79	2.00
15-16										36.5	9.79	4.72	3.33	1.92
16-17											15.6	6.42	3.55	2.23
17-18											32.5	8.11	4.52	2.45
18-19												14.1	5.78	2.80
19-20												28.9	7.57	3.13
20-21	MULTIPLY TABLE VALUES BY 10^{-4}												13.3	3.09
21-22													26.3	4.88
22-23														6.76
23-24														11.8
24-25														23.2
Avg. no. of electrons/cm^3 per photon/cm^2	3.79	3.29	2.92	2.64	2.38	2.19	2.02	1.81	1.61	1.45	1.33	1.21	1.14	1.05
	MULTIPLY VALUES BY 10^{-3}													

Table 4.6. Initial Compton electron-energy distribution in water (first-collision spectrum)

Number of electrons/(cm^3·MeV) per photon/cm^2

Electron energy interval (MeV)	Photon energy (Mev)							
	30	50	75	100	250	500	750	1000
0-1	1544	1019	719	559	264	169	101	77.1
1-5	88.4	27.7	10.8	8.97	1.56	0.539	0.216	0.112
5-10	95.8	35.7	13.6	8.60	1.43	0.452	0.173	0.0988
10-20	119	36.9	15.6	8.66	1.45	0.430	0.173	0.0972
20-30	520	44.5	17.2	8.59	1.49	0.448	0.153	0.102
30-40		64.2	19.7	9.03	1.44	0.431	0.161	0.0741
40-50		312	22.2	10.2	1.48	0.398	0.189	0.0787
50-60			31.9	12.1	1.42	0.438	0.149	0.103
60-70			66.2	13.7	1.31	0.394	0.127	0.106
70-80			169	17.6	1.57	0.452	0.183	0.0833
80-90				30.5	1.54	0.398	0.163	0.0849
90-100				155	1.50	0.401	0.175	0.0710
100-200					2.25	0.443	0.161	0.0890
200-300					9.37	0.523	0.167	0.0912
300-400						0.804	0.185	0.0958
400-500						6.23	0.242	0.102
500-600							0.325	0.119
600-700	MULTIPLY TABLE VALUES BY 10^{-4}						0.663	0.149
700-800							3.11	0.191
800-900								0.302
900-1000								2.62
Avg. no. of electrons/cm^3 per photon/cm^2	8.76	5.88	4.25	3.29	1.57	1.01	0.602	0.462
	MULTIPLY VALUES BY 10^{-3}							

Table 4.7. Initial positron-energy distribution in water (first-collision spectrum)

Number of positrons/(cm^3-MeV) per photon/cm^2

Electron energy interval (MeV)	Photon energy (MeV)													
	4	5	6	7	8	9	10	12	14	16	18	20	22	25
0-1	5.65	5.02	4.51	4.16	3.97	3.63	3.05	3.42	2.77	2.28	2.13	1.71	2.53	2.25
1-2	7.62	7.33	7.13	6.67	6.16	6.12	5.64	5.20	4.64	4.18	3.53	3.03	3.25	2.92
2-3	5.43	7.27	7.37	7.28	6.98	6.78	6.37	5.75	5.47	5.00	4.17	3.96	4.02	3.62
3-4		4.82	6.88	7.41	7.45	7.23	7.11	6.00	5.47	4.72	4.83	4.71	4.44	4.02
4-5			4.5[illegible]	7.00	6.90	7.27	7.30	5.97	5.52	5.40	4.85	4.32	4.15	3.78
5-6				4.24	6.22	6.84	6.93	5.96	5.74	5.30	5.27	5.02	4.52	4.02
6-7					3.66	5.74	6.25	5.84	5.44	5.39	5.00	4.89	4.32	4.15
7-8						3.28	5.25	5.89	5.65	5.17	5.05	4.57	4.31	3.89
8-9							2.96	5.65	5.58	5.45	4.93	4.99	4.07	4.01
9-10								5.14	5.09	5.05	5.32	4.84	4.10	3.81
10-11								3.41	4.94	5.25	4.72	5.09	4.05	4.27
11-12									4.75	4.91	5.19	4.48	4.31	3.80
12-13									2.84	4.88	4.74	5.10	4.07	4.34
13-14										4.10	4.42	4.81	4.08	3.90
14-15										2.34	4.61	4.37	4.45	3.82
15-16											3.79	4.24	4.05	3.92
16-17											1.97	4.13	4.06	4.16
17-18												3.23	4.07	3.95
18-19												1.71	4.10	3.77
19-20													3.70	3.76
20-21	MULTIPLY TABLE VALUES												2.38	3.92
21-22	BY 10^{-4}													3.71
22-23														3.28
23-24														2.08
24-25														0.00
Avg. no. of positrons/cm^3 per photon/cm^2	1.87	2.44	3.05	3.65	4.13	4.69	5.09	5.82	6.39	6.94	7.43	7.92	8.30	8.87
	MULTIPLY VALUES BY 10^{-3}													

Table 4.8. Initial positron-energy distribution in water (first-collision spectrum)
Number of positrons/(cm^3·MeV) per photon/cm^2

Electron energy interval (MeV)	Photon energy (MeV)							
	30	50	75	100	250	500	750	1000
0-1	1.88	1.60	1.21	1.03	0.817	0.394	0.244	0.184
1-5	3.15	2.24	1.46	1.07	0.701	0.317	0.183	0.124
5-10	3.57	2.54	1.80	1.34	0.739	0.332	0.180	0.146
10-20	3.59	2.41	1.95	1.51	0.741	0.373	0.206	0.122
20-30	2.83	2.36	1.81	1.52	0.767	0.393	0.244	0.146
30-40		2.50	1.82	1.53	0.774	0.373	0.254	0.175
40-50		2.08	1.86	1.51	0.702	0.417	0.244	0.169
50-60			1.92	1.50	0.716	0.414	0.265	0.193
60-70			1.85	1.53	0.674	0.410	0.291	0.196
70-80			0.492	1.53	0.695	0.425	0.268	0.180
80-90				1.53	0.629	0.365	0.281	0.209
90-100				0.972	0.627	0.380	0.284	0.215
100-200					0.646	0.365	0.269	0.209
200-300					0.362	0.341	0.254	0.203
300-400						0.370	0.246	0.199
400-500						0.385	0.245	0.195
500-600							0.265	0.193
600-700	MULTIPLY TABLE VALUES						0.281	0.201
700-800	BY 10^{-4}						0.106	0.203
800-900								0.214
900-1000								0.167
Avg. no. of positrons/cm^3 per photon/cm^2	0.965	1.17	1.33	1.43	1.71	1.85	1.92	1.96
	MULTIPLY VALUES BY 10^{-2}							

4.4 Comparisons with Other Work

As a check on the present calculations, results obtained with PHOEL-3 were compared in detail with the computations of Cormack and Johns (CJ52), who considered photon energies up to 25 MeV. Generally, very good agreemont was found. As expected, the differences were greatest at 25 MeV. Figure 4.1 shows a comparison of the present work with the Cormack and Johns results for the initial energy spectrum of all electrons and positrons produced by photons of this energy. The two calculations are different in that Cormack and Johns neglected Auger electrons and triplet production, which adds ∿5% to the total photon interaction cross section at 25 MeV. The curve in Fig. 4.1 from the present work is generally higher than that of Cormack and Johns, attributable to the use of slightly different pair-production cross sections and to the presence of triplet electrons, which add significantly to the relative number of low-energy electrons.

Similar comparisons were made with the somewhat later tables of Johns and Laughlin (JL56), which do include triplet production. Good agreement was found up to 25 MeV, where their calculations stopped.

The Cormack and Johns (CJ52) and the Johns and Laughlin (JL56) tables are the principal existing sources against which detailed checks of results calculated with PHOEL-3 can be made. Unfortunately, the comparisons are limited to photon energies not exceeding 25 MeV. Some differences with the existing tables are to be expected, since PHOEL-3 utilizes newer cross-section data and since the computations differ in certain details, such as the approximations used to handle triplet production. Such differences, like those found in Fig. 4.1, appear to be reasonable.

4.5 Applications to Dosimetry

PHOEL-3 utilizes basic physical data to provide a computer simulation of photon interactions that directly produce electrons and positrons in water. Applications of the data generated by the code were discussed in Section 1.3. This section describes how the numerical tables presented in this chapter can be used directly to obtain estimates of certain dosimetric quantities.

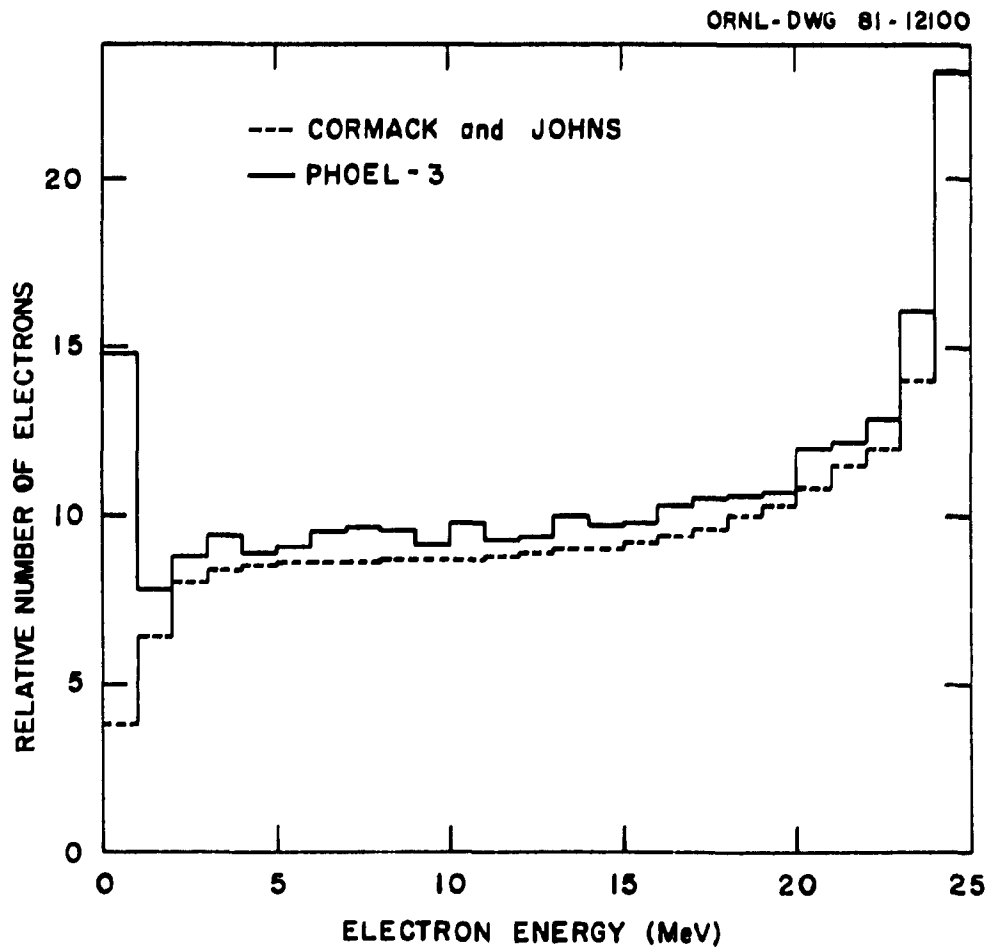

Fig. 4.1. Initial energy distribution of the total number of electrons and positrons produced by 25-MeV photons in water as computed with PHOEL-3 (solid histogram) and by Cormack and Johns (CJ52, dashed histogram). The difference in the two computations is consistent with the inclusion of triplet and Auger-electron production in PHOEL-3.

Kerma. Kerma is defined as the sum of the initial kinetic energies of all the charged particles liberated by indirectly ionizing particles in a volume element of a specified material divided by the mass of the volume element (IC80). The initial energies of any other charged particles, such as Auger electrons, produced in the volume element by secondary processes are also included in the kerma. In addition, it follows from this definition that any energy subsequently emitted by the charged particles in the form of bremsstrahlung is also included in the kerma. If all of the initial energy of the charged particles is absorbed in the volume element, then the kerma is equal to the absorbed dose in the element due to those interactions of the indirectly ionizing radiation.

The absolute spectra given in Tables 4.1-4.8 can be used to estimate kerma directly. Since multiple photon interactions were not considered in calculating the tables, the values given are proportional only to the "single-collision" or "first-collision" kerma. However, in many practical applications in dosimetry, the single-collision kerma is a good approximation to the kerma: e.g., in relatively small targets or in large targets at photon energies where the photoelectric effect or pair production dominates over Compton scattering.

We illustrate how the first-collision kerma can be estimated from the tables for a parallel beam of 70-keV photons incident on a 1-cm^3 water target. In this case, the kerma is almost exactly equal to the first-collision kerma. From Table 4.1 it is seen that, for unit photon fluence, (20.5×10^{-3} electrons/keV) x 5 keV = 0.1025 electrons are produced with energies between 0 and 5 keV. Assuming a mean energy of 2.5 keV gives for the kerma contribution from this group in water (unit density)

$$K_{0,5} = 0.1025 \times 2.5 = 0.256 \text{ keV/g} . \qquad (4\text{-}1)$$

Similarly, from the other 70-keV-photon entries in Table 4.1, one has

$$K_{5,10} = (8.60 \times 19^{-3}) \times 5 \times 7.5 = 0.311 \text{ keV/g} \qquad (4\text{-}2)$$

$$K_{10,15} = (11.5 \times 10^{-3}) \times 5 \times 12.5 = 0.719 \text{ keV/g} \qquad (4\text{-}3)$$

$$K_{15,20} = (0.202\times10^{-3}) \times 5 \times 17.5 = 0.018 \text{ keV/g} \quad (4\text{-}4)$$

$$K_{65,70} = (1.40\times10^{-3}) \times 5 \times 67.5 = 0.473 \text{ keV/g} \quad (4\text{-}5)$$

It follows that the total kerma is 1.78 keV/g per unit fluence of 70-keV photons.

If greater accuracy is desired, one can treat the Auger electrons and photoelectrons separately. Since the Auger electrons have an energy of only 0.508 keV (Section 2.2), the above calculation overestimates their effect on the kerma. Similarly, the photoelectron energy is 69.5 keV, rather than the assumed 67.5 keV; and so their effect on the kerma is underestimated. To correct for these approximations, we first find the number of electrons involved. Table 2.1 indicates that, at 70 keV, the ratio τ/μ of the photoelectric and total attenuation coefficients is 0.055. Thus, on the average, 0.055 photoelectrons and 0.945 Compton electrons are produced per photon interaction. Since all photoelectrons (Section 2.2) and 20% of the Compton recoil electrons (Section 2.3) leave a K-shell vacancy, an average of 0.055 + 0.2 (0.945) = 0.244 Auger electrons are produced per photon interaction. Therefore, the total fraction of electrons that are Auger electrons is 0.244/1.244 = 0.196. Since there are 0.211 electrons produced in the 1-cm^3 target per unit photon fluence (bottom entry in Table 4.1 for 70-keV photons), it follows that the number of Auger electrons is 0.196 x 0.211 = 0.0414. The kerma for these is

$$K_A = 0.0414 \times 0.508 = 0.0210 \text{ keV/g} \quad (4\text{-}6)$$

for water (unit density). Returning to the entry in interval 0-5 keV in Table 4.1, we have for the total number of electrons there 5 keV x 20.5×10^{-3}/keV = 0.103. Subtracting the number of Auger electrons leaves 0.103 - 0.0414 = 0.0611 other (i.e., Compton) electrons. Taking these to be evenly distributed in energy over the interval (mean energy = 2.5 keV) gives for their kerma

$$K_C = 0.0611 \times 2.5 = 0.153 \text{ keV/g} . \quad (4\text{-}7)$$

Adding (4-6) and (4-7) gives for the kerma in the lowest energy interval

$$K'_{0,5} = K_A + K_C = 0.174 \text{ keV/g} , \quad (4\text{-}8)$$

compared with the value 0.256 keV/g from Eq.(4-1) above. Similarly, for the photoelectrons we have, accurately,

$$K'_{65,70} = (1.4\text{x}10^{-3}) \text{ x } 5 \text{ x } 69.5 = 0.487 \text{ keV/g} . \quad (4\text{-}9)$$

Adding Eqs. (4-8), (4-2)-(4-4), and (4-9) gives for the total kerma K' = 1.71 keV/g per unit photon fluence, compared with the less accurate K = 1.78 keV/g obtained above.

Absorbed dose. The data in the tables can be used to obtain an estimate of absorbed dose in cases where (1) a first-collision dose is adequate and (2) the kerma and absorbed dose are equal. The first condition implies that the water target has dimensions which are not large compared with the mean free path of the photons. If bremsstrahlung is ignored, the second condition, on the other hand, implies that the target is large enough to absorb most of the secondary-electron energy. The dose is then uniform in the target. If significant bremsstrahlung energy escapes, then, of course, the kerma exceeds the absorbed dose. Even in this case, as we discuss at the end of this section, it may be possible to estimate bremsstrahlung losses and obtain the absorbed dose from the kerma. For the present we shall ignore bremsstrahlung and show the conditions under which the first-collision kerma is approximately equal to absorbed dose.

Figure 4.2 shows the attenuation and energy-absorption coefficients, μ and μ_A, respectively, for water for photons as functions of their energy. The quantities μ_{PE} and μ_{PP} are the photoelectric and pair-production attenuation coefficients; μ_{CS} and μ_{CA} are the Compton scattering and the Compton energy absorption coefficients. At 1 MeV, for example, the total attenuation coefficient is $\mu = 0.072 \text{ cm}^{-1}$, giving for the mean free path $1/\mu = 13.9$ cm. Compton scattering is the only photon interaction of importance at this energy, and the scattering and absorption coefficients are comparable. Because the mean free path is not greatly different from chord lengths in an anthropomorphic size phantom,

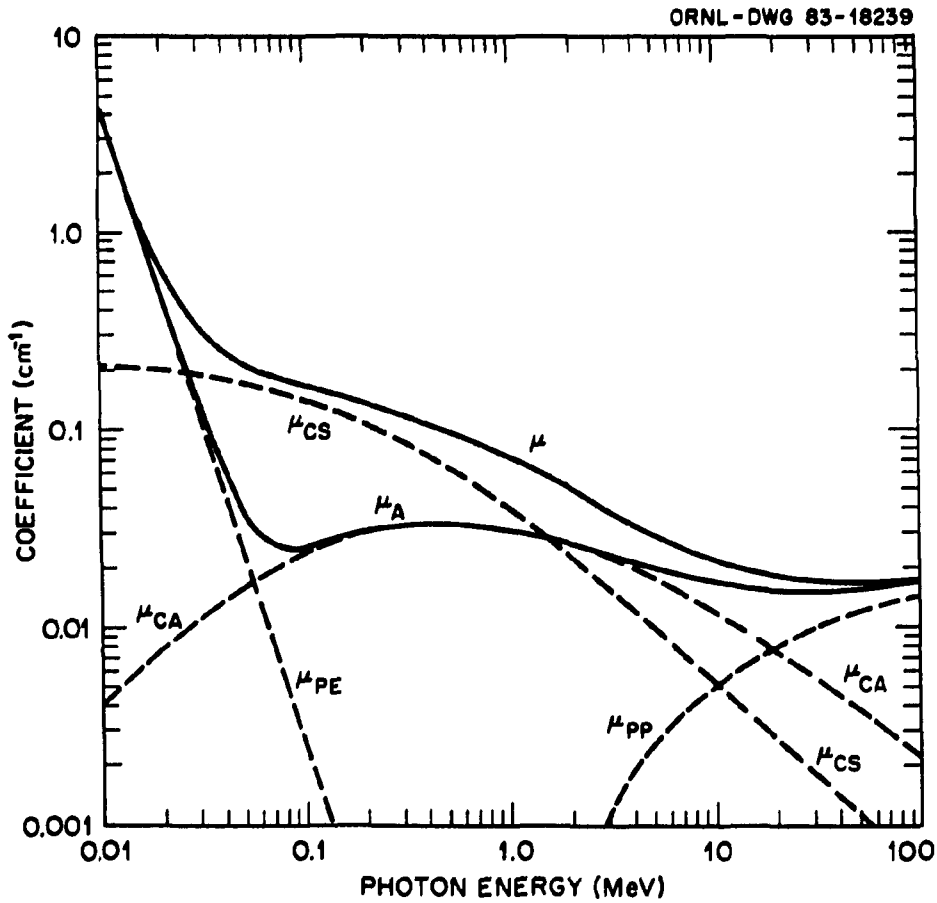

Fig. 4.2. Attenuation and energy-absorption coefficients, μ and μ_A, for photons in water as functions of energy. The component parts for the photoelectric effect (μ_{PE}), Compton scattering (μ_{CS}), Compton energy absorption (μ_{CA}), and pair production (μ_{PP}) are shown by the dashed curve.

the first-collision kerma provides a reasonable approximation to the kerma in man. Furthermore, in a phantom of this size, the kerma approximates the absorbed dose.

At photon energies above 1 MeV, μ decreases; and so the first-collision kerma becomes more nearly equal to the absorbed dose, until bremsstrahlung losses from the phantom become significant. Table 4.9 gives the relative value of the radiative stopping power of water to the total stopping power and the radiation yield for electrons (or positrons) of different energies. The radiation yield is the fraction of the initial electron energy that is emitted as bremsstrahlung when the electron is stopped completely. One sees from the table that the radiative and collisional stopping powers are equal at an electron energy just under 100 MeV and that the radiative yield is 50% for electrons just over 200 MeV in energy. Since the bremsstrahlung photon spectrum is approximately flat out to a maximum energy equal to the electron energy, not all of the bremsstrahlung energy will escape a man-sized phantom. As a rough rule-of-thumb, one could approximate the absorbed dose in a human phantom by taking the kerma minus half the radiation yield. In smaller targets, a larger fraction of the bremsstrahlung would escape. Bremsstrahlung is discussed in more detail below.

Table 4.9. Ratio of radiative and total stopping powers of water for electrons or positrons of different energies (NA64)

Electron energy (MeV)	Radiative stopping power / total stopping power	Radiation yield
1.0	0.009	0.005
10.0	0.084	0.042
50.0	0.346	0.190
100.0	0.522	0.317
200.0	0.689	0.467
500.0	0.847	0.659
1000.0	0.916	0.774

At photon energies below 1 MeV, the photon mean free path decreases rapidly due to the increasing cross section for Compton scattering; and at energies below 50 keV, it decreases due to the photoelectric effect (Fig. 4.). Multiple photon interactions occur over distances of several centimeters or less, and the dose distribution in a man-sized phantom is nonuniform. Unless the phantom is relatively small (e.g., a biological tissue-culture sample), the first-collision kerma can underestimate the absorbed dose by a considerable amount.

Radiation losses. We now describe how the radiation yield can be estimated as a function of electron or positron energy in a medium of effective atomic number Z (KM59). Koch and Wyckoff (KW58) represented the total electron energy loss per unit distance traveled by writing

$$-\frac{dE_o}{dx} = \frac{\rho Z}{A}\,(6 + 3.5\times10^{-3}\,E_o Z)\ , \qquad (4\text{-}10)$$

where E_o is the total initial electron energy in units of $m_o c^2$, ρ is the density of the target in g/cm^3, and A is the atomic weight. The first term in the parentheses represents the collision stopping power, and the second is the radiative stopping power. Integration from E_o down to the electron rest energy gives for the stopping distance

$$x_o = \frac{A}{3.6\times10^{-3}\,\rho Z^2}\,\ln(1 + 6\times10^{-4}\,ZE_o)\ . \qquad (4\text{-}11)$$

Since the collisional energy loss over x_o is $6\rho Z x_o/A$, the radiation yield is given by

$$\frac{E_o - 6\rho Z x_o/A}{E_o} = \frac{3\times10^{-4}\,ZT_o}{1 + 3\times10^{-4}\,ZT_o}\ , \qquad (4\text{-}12)$$

where T_o is the initial electron kinetic energy.

This method of estimating radiation yield utilizes a continuous slowing down approximation. Since the large fluctuations in radiative energy loss are not considered, the formula (4-12) is only approximate. In the absence of other information, however, it can be used to estimate the part of the kerma that is converted into bremsstrahlung.

4.6 Summary

The basic data presented here give the initial energies of electrons and positrons in water irradiated by monoenergetic photons with energies to 1 GeV. The tables have been designed for use for photons of an arbitrary energy spectrum by employing linear interpolation. The individual contributions from various physical processes are shown separately for some photon energies.

As described above, absolute values of the cross sections were used so that the tables contain the information with which to calculate the first-collision kerma per unit fluence of photons. In a wide range of dosimetric applications, the first-collision kerma for photons gives a good approximation to the absorbed dose. At high energies, where a significant fraction of the kerma is converted into bremsstrahlung, the approximate formula (4-12) for radiation yield enables one to estimate the part of the kerma that is not converted into absorbed dose.

REFERENCES

AN82 *Proceedings of the Workshop on the Interface between Radiation Chemistry and Radiation Physics, Argonne National Laboratory, Sept. 9-10, 1982*, Report ANL-82-88, Argonne, Illinois.

BA53 H. A. Bethe and J. Ashkin, "Passage of Radiations through Matter," *Experimental Nuclear Physics* (E. Segrè, Ed.), John Wiley, New York, 1953, Vol. I, Part II, pp. 166-357.

BM78 V. P. Bond, C. B. Meinhold and H. H. Rossi, "Low-Dose RBE and Q for X-Ray Compared to Gamma-Ray Radiations," *Health Phys.* 34, 433-438 (1978).

BN83 K. P. Beernink, R. F. Nelson and A. B. Chilton, "Consideration of Coherent Scattering and Electron Binding in Incoherent Scattering, in Computation of Dose Deposition in Tissue from Low-Energy Photon Beams," *Radiation Research* (in press).

BT53 C. D. Broyles, D. A. Thomas and S. K. Haynes, "The Measurement and Interpretation of the K Auger Intensities of Sn^{113}, Cs^{137}, and Au^{198}," *Phys. Rev.* 89, 715-724 (1953).

CJ52 D. V. Cormack and H. E. Johns, "Electron Energies and Ion Densities in Water Irradiated with 200 keV, 1 MeV and 25 MeV Radiation," *Brit. J. Radiol.* 25, 369-381 (1952).

DM75 G. Diambrini-Palazzi, E. Menichetti and A. Santroni, "On the Use of Coherent Electron-Pair Photoproduction and Bremsstrahlung Obtained from a 400 GeV Proton-Synchrotron," *Nucl. Instrum. Methods* 126, 369-372 (1975).

EV58 R. D. Evans, "Compton Effect," *Encyclopedia of Physics* (S. Flügge, Ed.), Springer Verlag, Berlin, 1958, Vol. 34, p. 218.

EV68 R. D. Evans, "X-Ray and Gamma-Ray Interactions," *Radiation Dosimetry* (G. J. Hine and G. L. Brownell, Eds.), Academic Press, Inc., New York, 1956, Chap. 3, pp. 93-155.

FN78 R. F. Ford and W. R. Nelson, *The EGS Code System: Computer Programs for the Monte Carlo Simulation of Electromagnetic Cascade Showers (Version 3)*, Report SLAC-210, Stanford Linear Accelerator Center, Stanford Univ., Stanford, Calif. (1978).

HB80 J. H. Hubbell, H. A. Gimm and I. Overbo, "Pair, Triplet and Total Atomic Cross Sections for 1 MeV-100 GeV Photons in Elements Z = 1 to 100," *J. Phys. Ref. Data* 9, 1023-1147 (1980).

HW78 R. N. Hamm, H. A. Wright, J. E. Turner and R. H. Ritchie, "Spatial Correlation of Energy Deposition Events in Irradiated Liquid Water," *Proceedings of Sixth Symposium on Microdosimetry, Brussels, Belgium, May 22-26, 1978* (J. Booz and H. G. Ebert, Eds.), Commission of the European Communities, Brussels, Belgium, 1978, pp. 179-186.

IC80 *Radiation Quantities and Units*, ICRU Report 33, International Commission on Radiation Units and Measurements, Washington, D.C. (1980).

JL56 H. E. Johns and J. S. Laughlin, "Interaction of Radiation with Matter," *Radiation Dosimetry* (G. J. Hine and G. L. Brownell, Eds.), Academic Press, Inc., New York, 1956, Chap. 2, pp. 49-123.

JM76 C. D. Jonah, M. S. Matheson, J. R. Miller and E. J. Hart, "Yield and Decay of the Hydrated Electron from 100 ps to 3 ns," *J. Phys. Chem.* 80, 1267-1270 (1976).

JM77 C. D. Jonah and J. R. Miller, "Yield and Decay of the OH Radical from 200 ps to 3 ns," *J. Chem. Phys.* 81, 1974-1976 (1977).

KM59 H. W. Koch and J. W. Motz, "Bremsstrahlung Cross-Section Formulas and Related Data," *Rev. Mod. Phys.* 31, 920-955 (1959).

KW58 H. W. Koch and J. W. Wyckoff, *IRE Trans. on Nucl. Sci.* NS-5(3) (1958).

MC83 P. J. McNulty, "Charged Particles Cause Microelectronics Malfunction in Space," *Phys. Today* 36(1), 9, 108-109 (1983).

MM66 A. Mozumder and J. L. Magee, "Model of Tracks of Ionizing Radiations for Radical Reaction Mechanisms," *Radiat. Res.* 28, 203-214 (1966).

NA64 *Studies in Penetration of Charged Particles in Matter* (U. Fano, Ed.), National Academy of Sciences-National Research Council, Washington, D.C., 1964, p. 249.

NC76 *Structural Shielding Design and Evaluation for Medical Use of X-Rays and Gamma Rays of Energies up to 10 MeV*, NCRP Report No. 49, National Council on Radiation Protection and Measurements, Washington, D.C. (1976).

NC77 *Radiation Protection Design Guidelines for 0.1-100 MeV Particle Accelerator Facilities*, NCRP Report 51, National Council on Radiation Protection and Measurements, Washington, D.C. (1977).

SW59 L. Slack and K. Way, *Radiations from Radioactive Atoms in Frequent Use*, U. S. Atomic Energy Commission, Washington, D.C., 1959.

TH78 J. E. Turner, R. N. Hamm, H. A. Wright, R. H. Ritchie and R. Katz, "Calculated Electron Slowing-Down Spectra for Liquid Water Irradiated by X and Gamma Rays--Implications for Photon RBE," *Proceedings of Sixth Symposium on Microdosimetry, Brussels, Belgium, May 22-26, 1978* (J. Booz and H. G. Ebert, Eds.), Commission of the European Communities, Brussels, Belgium, 1978, pp. 375-382.

TH80 J. E. Turner, R. N. Hamm, H. A. Wright, J. T. Módolo and G. M. A. A. Sordi, "Monte Carlo Calculation of Initial Energies of Compton Electrons and Photoelectrons in Water Irradiated by Photons with Energies up to 2 MeV," *Health Phys.* 39, 49-55 (1980).

TH82a A. S. Todo, G. Hiromoto, J. E. Turner, R. N. Hamm and H. A. Wright, "Monte Carlo Calculations of Initial Energies of Electrons in Water Irradiated by Photons with Energies up to 1 GeV," *Health Phys.* 43, 845-852 (1982).

TH82b A. S. Todo, G. Hiromoto, J. E. Turner, R. N. Hamm and H. A. Wright, *User's Manual for PHOEL-3, a Monte Carlo Computer Code for Calculating Initial Energies of Electrons in Water Irradiated by Photons with Energies up to 1 GeV*, Report ORNL/TM-8259, Oak Ridge National Laboratory, Oak Ridge, Tenn. (1982).

TM80 J. E. Turner, J. L. Magee, R. N. Hamm, A. Chatterjee, H. A. Wright and R. H. Ritchie, "Early Events in Irradiated Water," *Proceedings of Seventh Symposium on Microdosimetry, Oxford, U.K., Sept. 8-12, 1980* (J. Booz, H. G. Ebert and H. D. Hartfiel, Eds.), Commission of the European Communities, Brussels, Belgium, 1981, pp. 507-517.

TM83 J. E. Turner, J. L. Magee, H. A. Wright, A. Chatterjee, R. N. Hamm and R. H. Ritchie, "Physical and Chemical Development of Electron Tracks in Liquid Water," *Radiat. Res.* 96, 437-449 (1983).

TT82 A. S. Todo, J. E. Turner, R. N. Hamm and H. A. Wright, "Calculated Initial Energies of Electrons in Si and SiO_2 Irradiated by Photons with Energies up to 2 MeV," *Nucl. Instrum. Methods* 203, 459-465 (1982).

ORNL/TM-8987

INTERNAL DISTRIBUTION

1. K. F. Eckerman
2. R. N. Hamm
3-7. G. Hiromoto
8. S. V. Kaye
9. G. G. Killough
10-14. A. S. Todo
15-24. J. E. Turner
25. H. A. Wright
26-27. Central Research Library
28. Document Reference Section
29-30. Laboratory Records
31. Laboratory Records, RC
32. ORNL Patent Office
33-42. Radiation Shielding Information Center

EXTERNAL DISTRIBUTION

43-47. G.M.A.A. Sordi, Instituto de Pesquisas Energéticas e Nucleares, São Paulo, S. P., Brazil
48. J. N. Bradford, Hanscom Air Force Base, Massachusetts 01731
49. Office of Assistant Manager for Energy Research and Development, Oak Ridge Operations, Oak Ridge, Tennessee 37830
50-76. Technical Information Center, Oak Ridge, Tennessee 37830